NUMERICAL ANALYSIS OF CREEP AND SHRINKAGE BEHAVIOUR OF CONCRETE DURING LABORATORY TESTS USING ADVANCED CONSTITUTIVE MODEL

Daniela Šindelářová*[,1], Juraj Chalmovský[1]

*Daniela.Sindelarova@vutbr.cz
[1]Department of Geotechnics, Faculty of Civil Engineering, Brno University of Technology, Veveří 331/95, Brno

Abstract

This paper utilizes a time-dependent elastoplastic material model to predict the creep and shrinkage behaviour of laboratory samples via the Finite Element Method (FEM) analysis. After describing the time-dependent behaviour of concrete, the influence of creep input parameters of the material model is analysed in a parametric study. Finally, the values of creep and shrinkage input parameters are calibrated based on real tests and subsequent usage in the numerical modelling of geotechnical structures is discussed.

Keywords

Creep, shrinkage, calibration, finite element method, Plaxis 2D

1 INTRODUCTION

In some geotechnical applications, such as permanent retaining walls, the influence of time-dependent behaviour in concrete could have a significant impact on the long-term performance of the structure [1]. Creep and shrinkage not only contribute to increased deformation but also to the redistribution of internal forces [2]. Therefore, accurately captioning the time-dependent behaviour in geotechnical calculations is very important to predict the long-term behaviour of the construction.

Nowadays, permanent geotechnical constructions, such as diaphragm walls, can be designed based on finite element method calculations and employ advanced material models for surrounding materials (soils and rocks). For the material of the diaphragm walls themselves, linear elastic material models are usually used. This engineering approach neglects the influence of time-dependent behaviour, which can significantly impact the evaluation of deformations and stress in construction. Another engineering approach includes creep in long-term conditions but assumes the existence of only two conditions, short-term and long-term. The wall is in both conditions modelled using linear-elastic material models, and the wall's stiffness in short-term and long-term conditions is different [3].

The application of an advanced constitutive model for concrete offers the advantage of including continuous time-dependent behaviour in concrete as well as evaluating deformations and internal forces at every moment throughout the structure's lifetime.

This paper focuses on calibrating the creep and shrinkage behaviour of an advanced constitutive model for concrete [4] using datasets obtained from laboratory testing [5] and the finite element method software Plaxis 2D [6]. Results from this calibration can be further used in the numerical modelling of geotechnical structures [3].

2 METHODOLOGY

This paper consists of a brief description of the used material model [4], focusing on its time-dependent characteristics. Then, a parametric study was performed to analyse the influence of input creep parameters. Building upon the gained knowledge of the influence of the input creep parameters, the calibration of input parameters based on laboratory tests is then presented.

Time-dependent behaviour in concrete

The utilized material model (Shotcrete material model = SH model) [4], [7] was formally developed for modelling primary tunnel linings using the New Austrian Tunnelling Method (NATM). This material model can be used in various applications where it is necessary to include the influence of time-dependent behaviour in concrete. The current engineering approach of time-dependent analysis consists of step changes of the elasticity modulus in the calculation phases, and it is not able to realistically catch up with gradual changes in concrete and their influence on the construction behaviour.

This elastoplastic SH model [4] includes hardening and softening as well as time-dependent behaviour, including the development of strength, elasticity modulus, plasticity, creep and shrinkage, whereas the main objects of interest of this work are creep and shrinkage.

The increase in strength during concrete curing is defined according to Formula (1) where $f_{c,1}$ and $f_{c,28}$ are the concrete compressive strength (in kPa) after 1 day and 28 days of curing, respectively. Parameter $s_{strength}$ (dimensionless) governs the rate of increase in compressive strength and can be calculated using Formula (2).

Compressive strength $f_c(t)$ (in kPa) at a given the time t (in days), can be calculated using Formula (1).

$$f_c(t) = f_{c,28} \cdot e^{s_{strength}\left(1-\sqrt{28/t}\right)} \tag{1}$$

$$s_{strength} = -\frac{\ln\left(f_{c,1}/f_{c,28}\right)}{\sqrt{28}-1} \tag{2}$$

The compressive strength value after 28 days corresponds to the concrete strength class, and the recommended value of the ratio $f_{c,1}/f_{c,28}$ is between 0.2 and 0.3 [6].

The described compressive strength–time dependence for three different ratios $f_{c,1}/f_{c,28}$ is shown in Fig. 1. On the horizontal axis is the time in hours (logarithmic scale). On the vertical axis is the ratio of the actual compressive strength $f_c(t)$ and the final compressive strength $f_{c,28}$. Up to the first hour, the ratio of compressive strengths remains constant at zero, from the first hour until reaching the time of 28 days (672 hours), it follows a non-linear curve (1) and eventually it stabilizes at a value equal to 1, indicating that the actual compressive strength $f_c(t)$ equals the final compressive strength $f_{c,28}$.

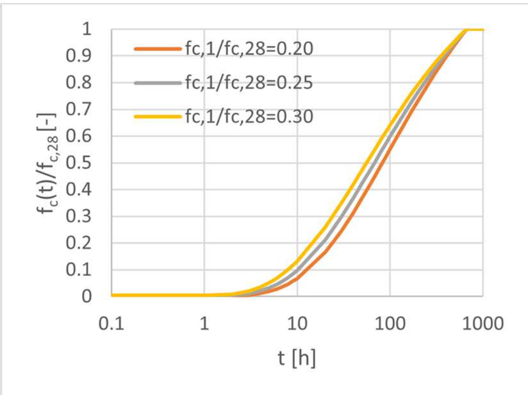

Fig. 1 The compressive strength – time dependence in the SH model.

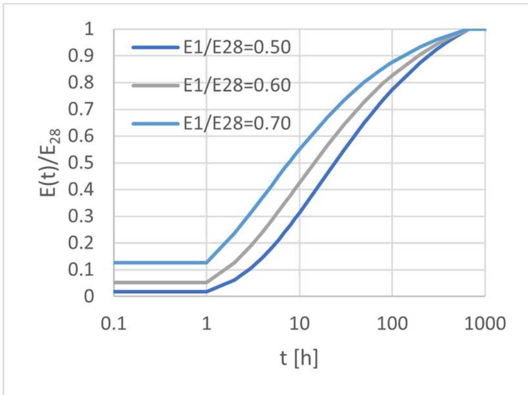

Fig. 2 The elasticity modulus – time dependence in the SH model.

The increase in Young's elasticity modulus over time, denoted as $E(t)$ in kilopascals (kPa) can be calculated using Formula (3) and mirrors the increase in compressive strength. The final value of the elasticity modulus after 28 days E_{28} (in kPa) corresponds to the concrete strength class. Another input parameter is the ratio between the modulus after 1 day and the modulus after 28 days (E_1/E_{28}). The elasticity modulus value after 28 days corresponds to the concrete strength class, and the recommended ratio E_1/E_{28} is between 0.5 and 0.7.

$$E(t) = E_{28} \cdot e^{s_{stiff}\left(1-\sqrt{28/t}\right)} \tag{3}$$

Parameter s_{stiff} (dimensionless) can be calculated using Formula (4), and the input parameter is the ratio E_1/E_{28}. E_1 is the Young's elasticity modulus (kPa) after 1 day.

$$s_{stiff} = -\frac{\ln(E_1/E_{28})}{\sqrt{28}-1} \tag{4}$$

DOI 10.13164/juniorstav.2024.24065

The described modulus – time dependence is shown for three different ratios E_1/E_{28} in Fig. 2. The horizontal axis represents time *t* in hours (logarithmic scale), while the vertical axis represents the ratio of the actual modulus *E(t)* to the final modulus E_{28}. Up to 1 hour, the ratio of the modulus is constant, then until the 28-day mark (672 hours), it follows a non-linear curve (3) after which it stabilizes at a value equal to 1, which means that the actual modulus *E(t)* is the same as the final modulus E_{28}.

The young concrete shows ductile behaviour with a high value of plastic ductility, which later rapidly decreases. In the used material model, plastic ductility is characterized by the parameter $\varepsilon_{cp}{}^{p}$. Three input values of this parameter at different time intervals - 1 hour $\varepsilon_{cp,1h}{}^{p}$, 8 hours $\varepsilon_{cp,8h}{}^{p}$ and 24 hours $\varepsilon_{cp,24h}{}^{p}$ - are considered. With these values, the progress of the plastic peak strain is illustrated in Fig. 3. The horizontal axis represents time *t* in hours (logarithmic scale), and the vertical axis the value of the plastic peak strain $\varepsilon_{cp}{}^{p}$.

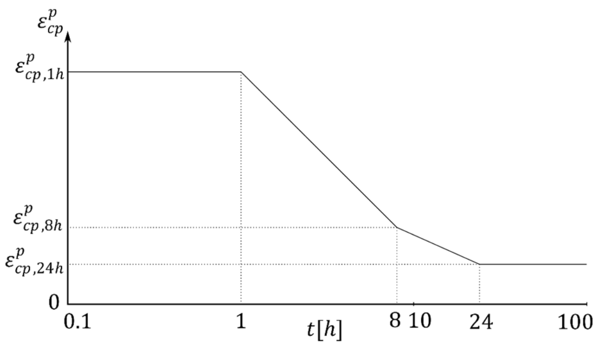

Fig. 3 The plastic peak strain-time dependence in the SH model.

Creep in the used material model [4] is defined by a viscoelastic element. The additional creep strain, $\varepsilon^{cr}(t)$ (dimensionless), at a given time *t* (in days) is defined according to Formula (5) where σ is the actual stress state (in kPa), *D* is the stiffness matrix (in kPa), and t_0 (in days) marks the beginning of the load application. The value of the creep strain is directly managed by two creep parameters ϕ^{cr} (ratio between creep and elastic deformation, dimensionless), and $t_{50}{}^{cr}$ (time in days required to achieve 50% creep strain). It is recommended to set the value of the creep factor in accordance with the standards [8] [9] [10], and the value of parameter $t_{50}{}^{cr}$ is recommended to be chosen within the range of 1 to 5 days [6].

$$\varepsilon^{cr}(t) = \frac{\varphi^{cr}\boldsymbol{\sigma}}{\boldsymbol{D}} \cdot \frac{t - t_0}{t + t_{50}^{cr}} \tag{5}$$

The definition of shrinkage in the used material model is similar to the definition of creep. There are two basic input parameters $\varepsilon_\infty{}^{shr}$ (final shrinkage strain, dimensionless) and $t_{50}{}^{shr}$ (time in days needed to achieve 50% of shrinkage strain). The actual shrinkage strain $\varepsilon^{shr}(t)$ (dimensionless) can be calculated using Formula (6). Shrinkage, unlike creep, is not dependent on the value of stress in the element, and the input variables in (6) are time *t* (in days) and shrinkage parameters $\varepsilon_\infty{}^{shr}$ and $t_{50}{}^{shr}$. Recommended values for $\varepsilon_\infty{}^{shr}$ range from -0.0002 to -0.0006, while for $t_{50}{}^{shr}$ range from 28 to 100 days [6].

$$\varepsilon^{shr}(t) = \varepsilon_\infty^{shr} \cdot \frac{t}{t + t_{50}^{shr}} \tag{6}$$

All the previously mentioned time-dependent phenomena interact in concrete together. The influence of the increase in strength and modulus can be neglected only in cases when the stress in the structure is applied after 28 days. As mentioned earlier, creep is stress-dependent, and the history of load application also plays a significant role. Shrinkage is independent of the load conditions and must be considered, especially during low-load, when the values of the creep strain and the shrinkage strain [3] are comparable.

Parametric study

A parametric study focusing on the influence of parameters governing creep behaviour was conducted. The FE model of the biaxial tests was prepared for this purpose. To evaluate the effect of creep parameters, shrinkage behaviour was not considered. The remaining parameters (Young's modulus, compressive strength, plastic ductility) were kept constant during the parametric study procedure.

This parametric analysis aimed to perform a set of calculations while using different combinations of the creep parameters ϕ^{cr} (1, 2.5, 4) and $t_{50}{}^{cr}$ (1, 3, 5 days), which led to 9 sets of input parameters (Tab. 1). Other material characteristics were chosen according to concrete classification C20/25, with compressive strength being 25 MPa,

DOI 10.13164/juniorstav.2024.24065

elasticity modulus 31 GPa, and density 25 kN/m^3. The value of the ratio $f_{c,1}/f_{c,28}$ was 0.43, and the ratio E_1/E_{28} was 0.65. Additional parameters were chosen considering recommendations [6].

Tab. 1 Variations of the creep parameters.

Var. no.	ϕ^{cr}	t_{50}^{cr}	Var. no.	ϕ^{cr}	t_{50}^{cr}	Var. no.	ϕ^{cr}	t_{50}^{cr}
1	*1*	*1*	*4*	*2.5*	*1*	*7*	*4*	*1*
2	*1*	*3*	*5*	*2.5*	*3*	*8*	*4*	*3*
3	*1*	*5*	*6*	*2.5*	*5*	*9*	*4*	*5*

The FE models consist of a squared sample with an edge length of 100 mm. The lower boundary was fully fixed, and the load was applied to the upper edge of the sample. This parametric study was divided into five stages, and every stage had different parameters (schedule and loading/unloading values), but in general, the phases of the calculations were similar (Tab. 2).

First, there was an Initial Phase with a specimen without any load. The second phase represents the time gap between the Initial Phase and the first load application. In the third phase, the load σ_L was applied, and throughout the fourth phase, it was kept constant. In the next phase, the applied load was decreased by the value of $\Delta\sigma$, and in the final phase, this reduced load was maintained.

Tab. 2 Phases of biaxial test.

Phase no.	Phase	Duration	Load
1	*Initial Phase*	*0*	*0*
2	*Concrete Curing*	t_1	*0*
3	*Load Application*	*0*	σ_L
4	*Loading*	t_2	σ_L
5	*Unloading*	*0*	$\sigma_L - \Delta\sigma$
6	*Observation*	t_3	$\sigma_L - \Delta\sigma$

Although the general concept of the biaxial test was similar, every stage of the parametric study had some specifics. The first stage examined the influence of the value of the applied load, and for this analysis, the stress in the specimen corresponded to 25%, 50% and 75% of the compressive strength at the moment of the load application. The second stage examined the influence of unloading, and the reduction of the load value was 25%, 50% and 75% of the load value. The remaining stages (stages three to five) varied in the duration of phases while the load value remained the same. The third stage modified the duration of the concrete curing before the first load application (1 day, 7 days, and 28 days). In this stage, the applied load was evaluated concerning the actual compressive strength at the moment of the load application (75%). The fourth stage varied in the duration of the load application before unloading (10 days, 25 days, and 40 days). During the fifth stage the duration of the observation after unloading was modified (25 days, 40 days, and 55 days). The complete scheme of the parametric study stages and variables is summarized in Tab. 3. Variables t_1, t_2, and t_3 represent the duration of the phases according to Tab. 2.

Tab. 3 Stages of parametric study.

Stage no.	Stage var.	t_1 [day]	t_2 [day]	t_3 [day]	$\sigma_L/f_c(t)$ [%]	$\Delta\sigma/\sigma_L$ [%]
1	*Loading*	*1*	*25*	*25*	*25 / 50 / 75*	*50*
2	*Unloading*	*1*	*25*	*25*	*75*	*25 / 50 / 75*
3	*First loading time*	*1 / 7 / 28*	*25*	*25*	*75*	*75*
4	*Loading duration*	*1*	*10 / 25 / 40*	*25*	*75*	*75*
5	*Observation duration*	*1*	*25*	*25 / 40 / 55*	*75*	*75*

In each of the five stages of this parametric study, a set of 27 calculations was performed (9 combinations of creep parameters, each evaluated for 3 calculation variations), leading to a total amount of 135 calculations. The focus of the numerical model was the middle point of the upper edge of the sample, and the measured quantity was the vertical displacement u_y (in mm) over time t (in days). For every calculation, a time-displacement curve was created, compared, and the summary results were subsequently formulated.

DOI 10.13164/juniorstav.2024.24065

Calibration on laboratory tests

A calibration of the long-term, time-dependent behaviour of the advanced constitutive model [4] was performed on the dataset obtained from published results of laboratory testing [5]. This study [5] was unique in its examination of creep and shrinkage behaviour in concrete in long-term conditions, and the calibration results are suitable for usage in further application. Compression test and four-point bending test were chosen for calibration. This calibration process aimed to replicate these laboratory tests using the finite element software and reach the values of the creep and shrinkage parameters in order to achieve the best agreement with results obtained from the laboratory testing [5].

The laboratory tests [5] were performed on concrete samples with a density of 24.1 kN/m^3, a compressive strength of 69.7 MPa and a Young's modulus of 41925 MPa. All specimens underwent curing for a period of 28 days under controlled conditions. To evaluate the influence on shrinkage, strains on unloaded samples were measured.

The compression test was performed on a cylinder with a base diameter of 110 mm and a height of 220 mm (Fig. 4). The specimen was loaded on the upper base, inducing a stress in the concrete equivalent to 50% of the compressive strength. This laboratory test was performed on two samples, yielding two sets of slightly different results. In the finite element software, this task was modelled in axisymetry mode (rectangle 55 × 220 mm). The active time-dependent behaviour consisted of an increase in compressive strength, elasticity modulus and creep. No control measurements on the unloaded samples for strain data were performed on this sample, and therefore no shrinkage strain data were available. Due to the high load level reached during the tests and the fact that strains due to creep depend on the actual stress state, additional strains due to shrinkage were assumed to be small compared to creep strains.

The phases of the compression test calibration are shown in Tab. 4 (C). The load value 34850 kN/m^2 applied on the upper edge of the calculation model was calculated to reach 50% of the compressive strength in the concrete.

This calibration test aimed to find the combination of such creep parameters which would give a curve closely matching the curves obtained from the laboratory testing. The observed point in the numerical model was the left point of the upper edge of the sample, with the measured quantity being a vertical strain in time *t* (in days).

Tab. 4 Phases of calibration tests (C = compression test, B = four-point bending test).

Phase no.	**Phase**	**Duration (C) [days]**	**Load (C) [kN/m^2]**	**Duration (B) [days]**	**Load (B) [kN/m^2]**
1	*Initial Phase*	*0*	*0*	*0*	*0*
2	*Concrete Curing*	*28*	*0*	*28*	*0*
3	*Load Application*	*0*	*34850*	*0*	*1080*
4	*Loading*	*216*	*34850*	*74*	*1080*
5	*Unloading*	*0*	*0*	*0*	*0*
6	*Observation*	*52*	*0*	*28*	*0*

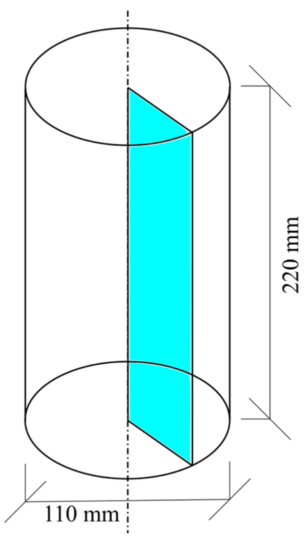

Fig. 4 Specimen for the compression test.

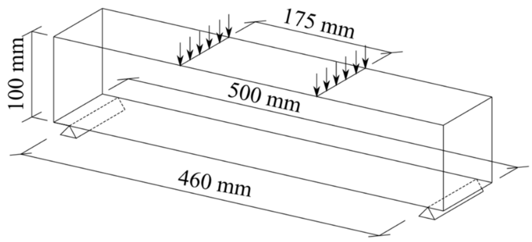

Fig. 5 Specimen for the four-point bending test.

DOI 10.13164/juniorstav.2024.24065

The four-point bending test was performed on a block 100 × 100 × 500 mm (Fig. 5). The applied load aimed to achieve a stress equal to 50% of the tensile strength on the outer fibres. In this particular test, the shrinkage behaviour played a significant role in strain development because the assumed range of shrinkage strain values was comparable to the range of values for both elastic and creep strain.

This laboratory test was performed on two samples, which gave two sets of slightly different results. In the finite element software, the task was modelled in plane strain mode (rectangle 500 × 100 mm). The applied load was adjusted to the equivalent load of 1 m. The supports and the load were considered as lines with a length of 50 mm. The active time-dependent behaviour consisted of an increase in compressive strength, elasticity modulus, creep, and shrinkage. Laboratory testing [5] included a control measurement on unloaded samples, and the results were used for the shrinkage behaviour calibration.

The phases of the four-point bending test calibration are shown in Tab. 4 (B). The load value 1080 kN/m^2 applied on the two places on the upper edge of the calculation model was calculated to reach 50% of the tensile strength in the concrete.

First, the shrinkage behaviour parameters were calibrated. Next, the calibration test aimed to find the combination of the creep parameters that results in a curve best matching two curves obtained from the laboratory testing. The observed points of the numerical model were the middle point of the upper edge and the middle point of the lower edge of the sample. The measured quantity was horizontal strain over time *t* (in days).

3 RESULTS

Parametric study

Throughout the entire parametric study, a total of 135 calculations were performed, and corresponding time-displacement curves were created. In this chapter, two representative graphs are presented. The influence of the ϕ^{cr} input parameter for t_{50}^{cr} = 5 days and various load levels σ_L are shown in Fig. 6. The influence of the ϕ^{cr} input parameter for t_{50}^{cr} = 5 days and various time of the first loading t_1 are shown in Fig. 7.

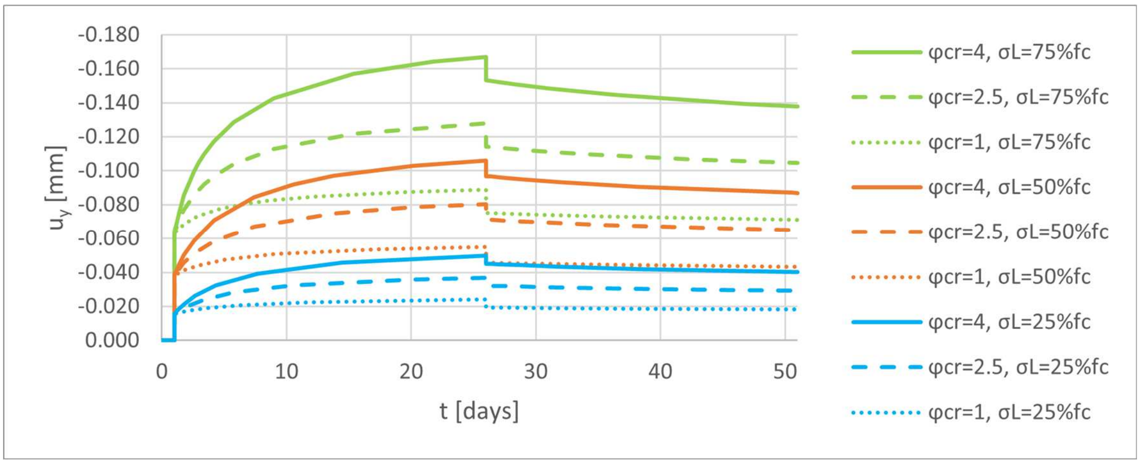

Fig. 6 Influence of the load value and ϕ^{cr} (t_{50}^{cr} = 5 days).

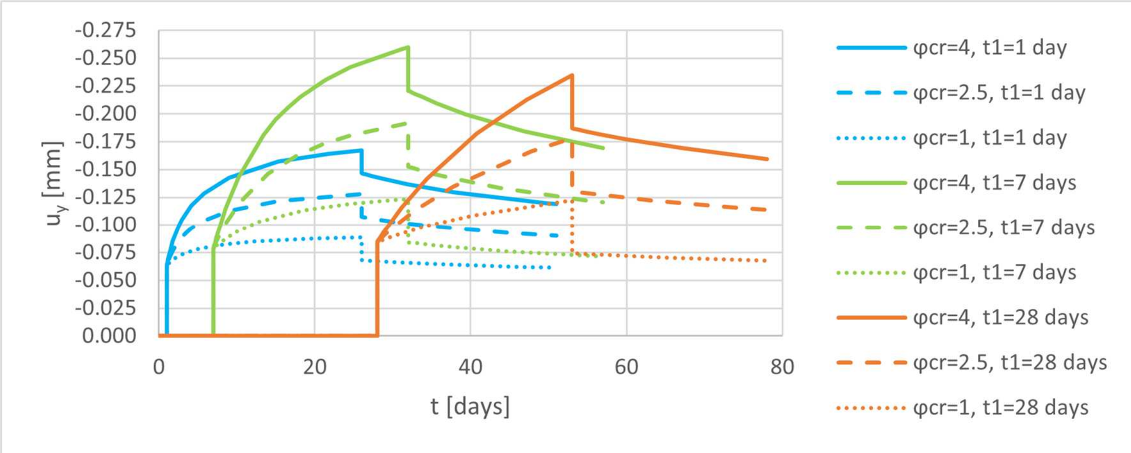

Fig. 7 Influence of the first loading time and ϕ^{cr} (t_{50}^{cr} = 5 days).

Calibration on laboratory tests

Time-strain curves were created for both the compression test (Fig. 8) and the four-point bending test (Fig. 9) and were then compared with the curves obtained from the laboratory tests [5]. The combination of creep and shrinkage parameters showing the best results are presented in Tab. 5.

Tab. 5 Calibration results.

Test	ϕ^{cr} [-]	t_{50}^{cr} [days]	$\varepsilon_{\infty}^{shr}$ [-]	t_{50}^{shr} [days]
Compression	*1.1*	*10*	-	-
Four-point bending	*0.8*	*40*	$-2.8 \cdot 10^{-5}$	*86*

The final curves are presented in Fig. 8 and Fig. 9. Dashed lines are the curves obtained from the laboratory testing.

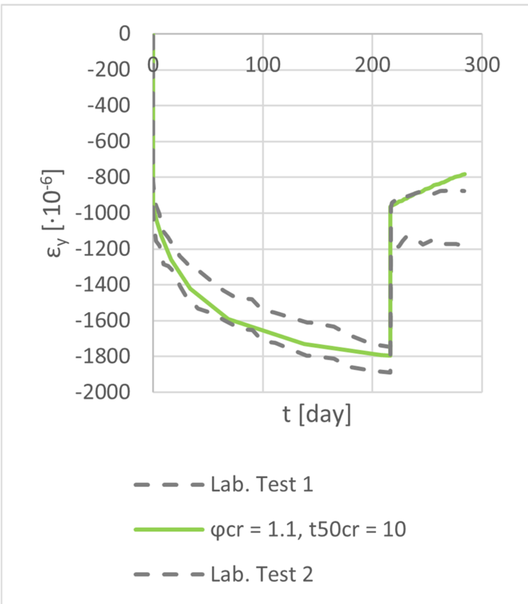

Fig. 8 Calibration results – compression test.

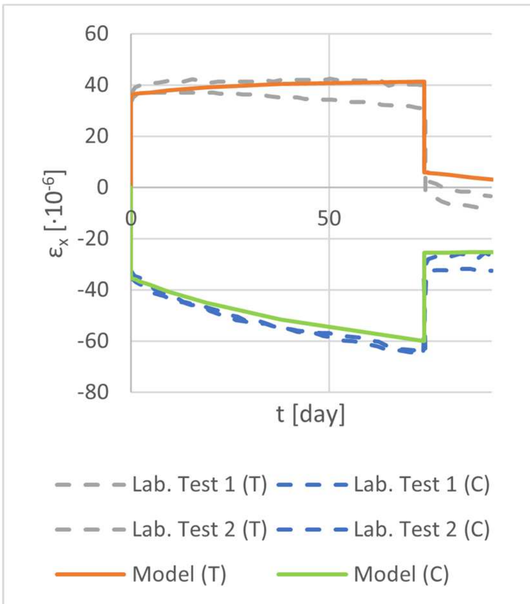

Fig. 9 Calibration results – four-point bending test.

DOI 10.13164/juniorstav.2024.24065

4 DISCUSSION

The parametric study investigating the influence of the values of input creep parameters obtained the following results:

- The value of the creep parameters is not related to the achieved value of the elastic strain. Elastic strain is a function of stress and the elastic modulus.
- The parameter ϕ^{cr} affects the final value of the creep strain, and the parameter t_{50}^{cr} modifies the creep rate of increase. With the higher ϕ^{cr}, the final creep strain value increases. With the higher t_{50}^{cr}, the rate of strain decreases.
- After unloading, creep deformation in the reverse direction increases with increasing ϕ^{cr} values.
- The time of the first load application significantly affects the creep strain increase. In young concrete (with the same value of t_{50}^{cr}), the rate of creep strain increase is higher.

This parametric study showed the influence of creep parameters on a time-dependent behaviour. Considering the range of recommended values [6], time-strain curves were significantly different. Before utilization of this material model for application in real-world scenarios, it is necessary to perform laboratory tests and time-dependent behaviour calibration.

For the compression and the four-point bending test, creep and shrinkage parameters best matching the laboratory testing results were different, as shown in Tab. 5. The differences might be caused by the absence of a control measurement on the unloaded specimens. Attempts to use calibrated shrinkage parameters from the specimen for the four-point test in the calibration of the compression test were not possible due to different sample dimensions (causing different shrinkage behaviour). Another possible reason for this difference was the total duration of the laboratory test. While, in the compression test, the load was maintained for 216 days in the four-point bending test the load was maintained for a shorter period of only 72 days.

While both of the calibration tests showed agreement with the laboratory test results in the loading part of curves, differences were present in the unloading part of the curves. After unloading elastic deformation, the numerical model showed faster deformation development than the laboratory test results.

For further research, more data from laboratory testing will be needed. These data should consider the long-term character of the test and should provide information about shrinkage and the progression of the compressive strength increase for every set of specimens. The data source from the laboratory testing [5] worked with high-strength concrete, so further research could use concrete with standard compressive strength to ensure the best possible alignment with the materials used in real constructions. All laboratory tests were performed on plain concrete without reinforcement, the next stage of the research should include this factor.

The four-point bending test due to its valuable results is suitable for further utilization in real-world applications (diaphragm wall) because of the strain values and stress range.

5 CONCLUSION

This study used the advanced constitutive elastoplastic model [4] for concrete to predict time-dependent behaviour via the finite element method, with an emphasis on creep deformation.

The parametric analysis of the influence of the input creep parameters and calibration of the material model gave the following results.

- Creep and shrinkage parameters do not influence elastic deformation.
- The parameter ϕ^{cr} determines the final value of the creep deformation. The value reached from the calibration is slightly lower than the recommended value [6], [10].
- The parameter t_{50}^{cr} determines the speed of creep deformation increase. The value reached from the calibration is (in long-term conditions) higher than the recommended value [4], [6].
- The time of first loading significantly influences the rate of creep deformations with higher values observed in ‘young’ concrete.
- Shrinkage behaviour must be considered, especially in low-load conditions.
- Creep occurs in both compression and tension. In tension the effects of creep and shrinkage are opposite, and superposition is used to calculate the total deformation at a given time.

After calibration, the advanced constitutive model [4] can be used in the solution of real boundary problems, providing an effective way to consider the time-dependent behaviour in long-term conditions.

DOI 10.13164/juniorstav.2024.24065

For further research it is recommended to conduct more long-term laboratory testing on cast concrete samples with shrinkage control measurements on the unloaded samples. Additionally, the next stage of this research could focus on the influence of reinforcement in cast concrete on the time-dependent behaviour.

Acknowledgement

This paper proceeded within the PhD study in the Faculty of Civil Engineering, BUT.

References

[1] ARBOLEDA-MONSALVE L.G. FINNO R.J. Influence of Concrete Time-Dependent Effects on the Performance of Top-Down Construction. *Journal of Geotechnical and Geoenvironmental Engineering* [online]. 2015, vol. 141, no. 4. [accessed 6 October 2023]. ISSN 1943-5606. Available at: https://doi.org/10.1061/(ASCE)GT.1943-5606.0001260

[2] GHOSH S.K. COHN M.Z. Effect of creep on the flexural strength and deformation of structural concrete. IABSE reports of the working commissions [online]. 1970, vol. 5. [accessed. 6 October 2023]. Available at: https://doi.org/10.5169/seals-6925

[3] ŠINDELÁŘOVÁ, Daniela. Modelování podzemních stěn pomocí časově závislého elasto-plastického materiálového modelu [online]. Brno, 2022. Thesis. Brno University of Technology, Faculty of Civil Engineering. Supervised by Juraj Chalmovský. Available at: https://www.vut.cz/www_base/zav_prace_soubor_verejne.php?file_id=235377

[4] SCHÄDLICH B. SCHWEIGER H.F. A new constitutive model for shotcrete [online]. Computational Geotechnics Group. Austria: Institute for Soil Mechanics and Foundation Engineering, Graz University of Technology, 2014. Available at: http://dx.doi.org/10.1201/b17017-20

[5] RANAIVOMANANA N. MULTON S. TURATSINZE A. Basic creep of concrete under compression, tension and bending. *Construction and Building Materials* [online]. 2013, no. 38, pp. 173–180. ISSN 0950-0618. Available at: https://dx.doi.org/10.1016/j.conbuildmat.2012.08.024

[6] PLAXIS Materials Model Manual 2019: Plaxis bv, Bentley Systems, Incorporated, 2019. ISBN-13: 978-90-76016-27-6

[7] SCHÜTZ R. POTTS D.M. ZDRAVKOVIC L. Advanced constitutive modelling of shotcrete: Model formulation and calibration. *Computers and Geotechnics* [online]. 2011, vol. 38, no. 6, pp. 834–845. ISSN 0266-352X. Available at: https://doi.org/10.1016/j.compgeo.2011.05.006

[8] CEB-FIP model code. Design code – comite Euronational du Beton. London: Thomas Telford, 1990

[9] EN 14487-1:2022. Sprayed concrete – Part 1: Definitions, specifications and conformity. Brussels, European Committee for Standardization, 2022

[10] EN 1992-1-1: 2004+A1:2014. Eurocode 2: Design of concrete structures – General rules and rules for buildings. Brussels, European Committee for Standardization, 2014